ISSN: 0067-2904

Electroosmosis Augmented MHD Peristaltic Transport of SWCNTs Suspension in A Porous Media

Hana Ibrahim Lafta[1*] , Ahmed M. Abdulhadi[2], Mizal Hamad Thawi[3]
[1]*Department of Mathematics, College of Computer Science and Mathematics, Tikrit University, Tikrit, Iraq.*
[2]*Department of Mathematics, College of Sciences, University of Baghdad, Baghdad, Iraq.*
[3]*Department of Mathematics, College of Computer Science and Mathematics, Tikrit University, Tikrit, Iraq.*

Received: 22/9/2022 Accepted: 5/5/2023 Published: 30/5/2024

Abstract

In this article, we analyses electroosmosis augmented MHD peristaltic transport of SWCNTs suspension in porous media, the basic equations have been constructed under assumptions of low Reynolds number and long wave length. The exact solution by the regular perturbation technique are obtained and the flow qualities have been plotting by using MATHEMATICA software for all the figures. Series solution for stream function, pressure gradient and temperature distribution have been computed in the peristaltic transport in an asymmetric channel.

Keywords: Electroosmosis, Magnetohydrodynamic, Peristaltic transport, Asymmetric channel, Porous media, Pressure gradient.

التوسيع التناضحي–الكهربي المعزز بالنقل التمعجي المغنطيسي الهيدروديناميكي للأنابيب النانوية المعلقة في وسط مسامي (SWCNTs) الكربونية أحادية الجدار

هناء ابراهيم لفته[1*]، أحمد مولود عبد الهادي[2]، مزعل حمد ثاوي[3]
[1] قسم الرياضيات، كلية علم الحاسوب والرياضيات، جامعة تكريت، تكريت، العراق.
[2] قسم الرياضيات، كلية العلوم، جامعة بغداد، بغداد، العراق.
[3] قسم الرياضيات، كلية علم الحاسوب والرياضيات، جامعة تكريت، تكريت، العراق.

الخلاصه

في هذه المقالة ، نقوم بتحليل التوسيع التناضحي–الكهربي المعزز بالنقل المغنطيسي الهيدروديناميكي ، التمعجي لتعليق الأنابيب النانوية الكربونية أحادية الجدار (SWCNTs) في الوسائط المسامية ، تم بناء المعادلات الأساسية على افتراضات انخفاض عدد رينولدز وطول الموجة الطويلة. تم الحصول على الحل الدقيق بتقنية الاضطراب العادية وتم رسم صفات التدفق باستخدام برنامج MATHEMATICA لجميع الأرقام. تم حساب الحل المتسلسل لدالة التدفق وتدرج الضغط وتوزيع درجة الحرارة في النقل التمعجي في قناة غير متماثلة.

*Email: hanaibra2022@gmail.com

1. Introduction

Electroosmosis is well known process in which the movement of liquids from less concentrated solution to more concentrated solution under the influence of the electric field [1].

Electroosmosis is the flow of liquid that is contact with a charged solid surface when an electric field is applied, and it becomes an important consideration with the increased surface area to volume ratio associated with small diameter capillaries [2]. This phenomena have many applications in medical diagnostics, drug delivery, chemical analysis, and environmental detection [3]. Many works on electroosmosis in various phenomena such as the thermodiffusion in aqueous solutions, thermomigration, movement of ions and nanochannels have been considered [4].

The magnetohydrodynamic MHD phenomenon is characterized by an interaction between the hydrodynamic and boundary layer and the electromagnetic field [5]. The studies of boundary layer flows of viscous and non-Newtonian fluids over a stretching surface have received much attention because of their extensive applications in the field of metallurgy and chemical engineering, for example, in the extrusion of polymer sheet from a dye. Such investigations of MHD flows are very important industrially and have applications in different areas of researches such as petroleum production and metallurgical processes, it is now well known that in technological applications the non-Newtonian fluids are more appropriate than the Newtonian fluids [6]. The word peristaltic comes from the Greek word "peristaltikos" which means clasping and compressing [7]. The phenomenon of peristaltic transport is defined as the expansion and contraction of an extensible tube in a fluid generate progressive waves which propagate along the length of the tube, mixing and transporting the fluid in the direction of wave propagation [8]. It plays an indispensable role in transporting many physiological fluids in the body in various situations, such as Urine transport from the kidney to the bladder through the ureter, transport of bile in the bile duct, and many bio-mechanical and engineering devices have been designed on the basis of the principle of peristaltic pumping to transport fluids without internal moving parts [9]. There are many researchers discussed the peristaltic transport with MHD field effects currently, the combined effects of electroosmosis and porous media receive considerable attention due to its application in the salty springs in the sea, in reservoir engineering in connection with thermal recovery, in the chemical industry and other [10]. In this work, electroosmosis augmented MHD peristaltic transport of SWCNTs suspension in porous media has been investigated. The constitutive equations are used to find the stress components substituted in the relevant flow problem that modeled with respect to Cartesian coordinates, and simplified by using the long wavelength and low Reynolds number approximation in to high non-linear partial differential equation that solved analytically by employing the regular perturbation technique for stream function, pressure gradient and temperature in MATHEMATICA software. The influences of all parameters in the flow expression are plotted and discussed in detail.

2. Mathematical Formulation

In this portion, a brief summary of the problem, electroosmosis augmented MHD peristaltic transport of SWCNTs suspension in porous media, in an asymmetric channel having a total width of "$d_1 + d_2$". Consider $\bar{x}$ and $\bar{y}$ axises along and vertical to the flow, the velocity components $(\bar{u}\,, \bar{v})$ along $(\bar{x}\,, \bar{y})$ directions respectively, as shown in Figure 1.

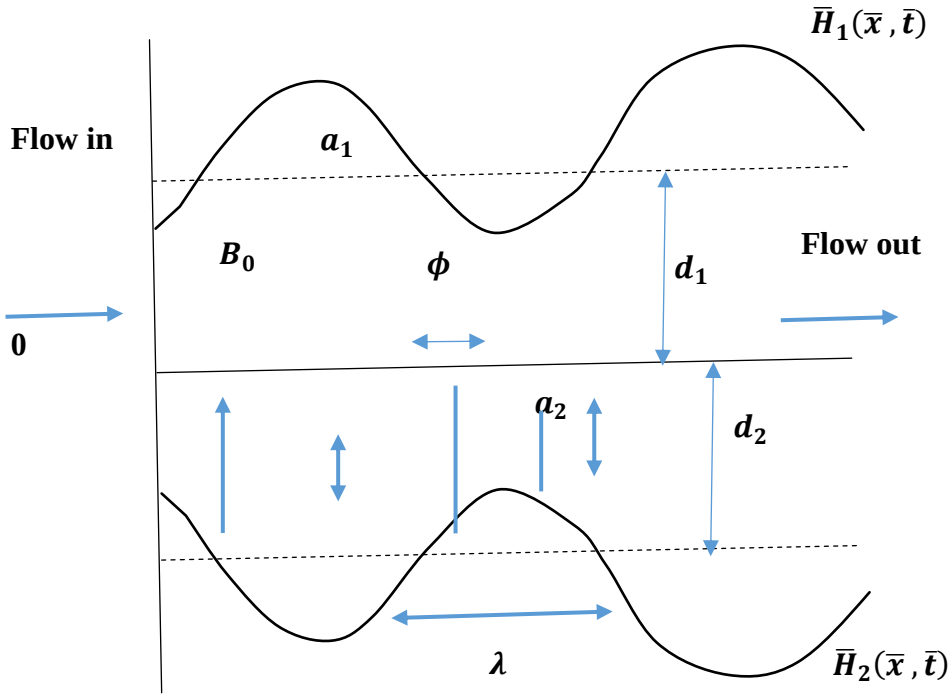

Figure 1: Diagrammatic of the problem.

The mathematical model of a symmetric channel with a constant speed c can be expressed as follows:

$$H_1 = d_1 + a_1 \sin\left(\frac{2\pi}{\lambda}(\bar{x} - c\bar{t})\right) \quad for\ upper\ wall$$
$$H_2 = -d_2 - a_2 \sin\left(\frac{2\pi}{\lambda}(\bar{x} - c\bar{t}) + \Phi\right) \quad for\ lower\ wall \tag{1}$$

where d_1; d_2 represent the half-width of the channel, a_1; a_2 are the wave amplitudes; c is the wave speed; $\bar{t}$ is the time; λ is the wavelength, H_1; H_2 are the transverse displacement of the upper and lower wall, respectively; and Φ the phase difference which lies between zero to π. The fluid is electrically conducting in the presence of an applied magnetic field B_0 in transverse direction to the flow. Magnetic Reynolds number is taken small and thus the induced magnetic field neglected, and d_1; d_2 ; a_1; a_2; and Φ satisfy the relation:

$$(d_1 + d_2)^2 \geq a_1^2 + a_2^2 + 2a_1 a_2 \cos\Phi$$

3. Basic and Governing Equations

The constitutive equations for current flow problem subject to considered flow conditions can be summarized as:

Continuity Equation

$$\frac{\partial \bar{u}}{\partial \bar{x}} + \frac{\partial \bar{v}}{\partial \bar{y}} = 0$$

Motion Equations

$$\rho_{nf}\left(\frac{\partial \bar{u}}{\partial \bar{t}} + \bar{u}\frac{\partial \bar{u}}{\partial \bar{x}} + \bar{v}\frac{\partial \bar{u}}{\partial \bar{y}}\right) = -\frac{\partial \bar{P}}{\partial \bar{x}} + \mu_{nf}\left(\frac{\partial^2 \bar{u}}{\partial \bar{x}^2} + \frac{\partial^2 \bar{u}}{\partial \bar{y}^2}\right) - \frac{\mu_{nf}}{k}\bar{u} - \sigma B_0^2 \bar{u} + \rho_e E_{\bar{x}} + (\rho\gamma)_{nf} g(\bar{T} - \bar{T}_0)$$

$$\rho_{nf}\left(\frac{\partial \bar{v}}{\partial \bar{t}}+\bar{u}\frac{\partial \bar{v}}{\partial \bar{x}}+\bar{v}\frac{\partial \bar{v}}{\partial \bar{y}}\right) = -\frac{\partial \bar{P}}{\partial \bar{y}}+\mu_{nf}\left(\frac{\partial^2 \bar{v}}{\partial \bar{x}^2}+\frac{\partial^2 \bar{v}}{\partial \bar{y}^2}\right)-\frac{\mu_{nf}}{k}\bar{v}-\sigma B_0^2\bar{u}+\rho_e E_{\bar{y}}$$

And, we get:

$$\frac{\partial \bar{T}}{\partial \bar{t}}+\bar{u}\frac{\partial \bar{T}}{\partial \bar{x}}+\bar{v}\frac{\partial \bar{T}}{\partial \bar{y}}=\alpha_{nf}\left(\frac{\partial^2 \bar{T}}{\partial \bar{x}^2}+\frac{\partial^2 \bar{T}}{\partial \bar{y}^2}\right)+\tau L^T-\frac{\partial q_r}{\partial \bar{y}} \quad (2)$$

where, L =grad $(\bar{v})$, the fluid velocity gradient in the Cartesian coordinated system $(\bar{x}\,,\bar{y})$ and L^T is the transpose of the fluid velocity gradient in the Cartesian coordinated system $(\bar{x}\,,\bar{y})$. The radiative heat flux (q_r) which is characterized by Rosseland approximation, assuming that heat flux is dominate in $\bar{y}$-direction only as [11]:

$$q_r=\frac{-16\bar{\sigma}\bar{T}_0^3}{3k^*}\frac{\partial \bar{T}}{\partial \bar{y}} \quad (3)$$

where, $\bar{\sigma}$ specifies the electric conductivity; k^* is the Rosseland mean absorption; $\bar{P}$ the pressure; $(\rho\gamma)_{nf}$ the effective thermal expansion of nano liquid; ρ_{nf} the effective density of nano liquid; ρ_e the charge number density; $\bar{E}_{\bar{x}}$ and $\bar{E}_{\bar{y}}$ are the electro kinetic body force in $\bar{x}$ and $\bar{y}$ directions; τ is the stress tensor; μ_{nf} the effective thermal diffusivity of nano liquid; k the permeability of porous medium, furthermore; T is the temperature of the material. The effective thermal conductivity of CNT suspension is described by xue model is given as [12]:

$$\rho_{nf}=(1-\Phi)\rho_b+\Phi\rho_{SWCNT} \quad , \quad \mu_{nf}=\frac{\mu_b}{(1-\Phi)^{2.5}}$$

$$\left(\rho c_p\right)_{nf}=(1-\Phi)\left(\rho c_p\right)_b+\Phi\left(\rho c_p\right)_{SWCNT} \quad , \quad \alpha_{nf}=\frac{k_{nf}}{\left(\rho c_p\right)_{nf}}$$

$$\frac{k_{nf}}{}=\frac{(1-\Phi)+2\Phi\frac{k_{SWCNT}}{k_{SWCNT}-k_b}\ln\left(\frac{k_{SWCNT}+k_b}{2k_b}\right)}{(1-\Phi)+2\Phi\frac{k_b}{k_{SWCNT}-k_b}\ln\left(\frac{k_{SWCNT}+k_b}{2k_b}\right)} \quad (4)$$

where ρ_b being the density of water; ρ_{SWCNT} the density of single-wall carbon nano tubes; k_b and k_{SWCNT} the thermal conductivity of water and SWCNTs, respectively; and Φ the volume fraction of SWCNTs.

Electrohydrodynamics EHD

Electrohydrodynamics or electrokinetics, is the study of dynamics of electrically charged fluids, that means study of motions of ionized particles or molecules and their interaction with electric fields and the surrounding fluid [13]. Poisson equation is utilized to characterize the electric potential (Φ) generated across EDL as [14]:

$$\nabla^2\Phi=-\frac{\bar{\rho}_e}{\epsilon_0} \quad (5)$$

where, ρ_e denotes the electric charge number density is written by:

$$\bar{\rho}_e=ez(\bar{n}^+-\bar{n}^-) \quad (6)$$

Where, e specifies electric charge, z denoted the charge balance of ionic species, $\bar{n}^+$and $\bar{n}^-$ are the number of densities of positive cations and negative anions respectively. Also, the

result of potential distribution depends on the charge number density. Then, the distribution of ions within the fluid is described by employing Nernst-Planck equation [15], which is:

$$\left(\frac{\partial \bar{n}^{\pm}}{\partial \bar{t}}+\bar{U}\frac{\partial \bar{n}^{\pm}}{\partial \bar{x}}+\bar{V}\frac{\partial \bar{n}^{\pm}}{\partial \bar{y}}\right)=D_m\left(\frac{\partial^2 \bar{n}^{\pm}}{\partial \bar{x}^2}+\frac{\partial^2 \bar{n}^{\pm}}{\partial \bar{y}^2}\right)\pm\frac{D_m ez}{\bar{T}_e k_B}\left[\frac{\partial}{\partial \bar{x}}\left(\bar{n}^{\pm}\frac{\partial \bar{\Phi}}{\partial \bar{x}}\right)+\frac{\partial}{\partial \bar{y}}\left(\bar{n}^{\pm}\frac{\partial \bar{\Phi}}{\partial \bar{y}}\right)\right] \quad (7)$$

where, k_B, T_e, and D_m assign the Boltzmann constant, the average temperature of the electrolytic solution and the diffusion coefficient.

3.1 Dimensionless Parameters

To create the governing equations non-dimensions, it is convenient to introduce the following non-dimensional variables and parameters:

$$\bar{H}_1=h_1 d_1\ ,\ \bar{H}_2=h_2 d_2\ ,\ a=\frac{a_1}{d_1}\ ,\ b=\frac{a_2}{d_2}\ ,\ \delta=\frac{d}{\lambda}\ ,\ \bar{x}=\lambda x\ ,\ \bar{y}=yd\ ,\ \bar{u}=cu\ ,\ \bar{v}=cv\ ,$$
$$\bar{n}=nn_0\ ,\ \bar{p}=\frac{p\mu_0 c}{d}\ ,\ \theta=\frac{\bar{T}-\bar{T}_0}{\bar{T}_0}\ ,\ P_r=\frac{\mu_b c_p}{k_b}\ ,\ L=\frac{(\rho\gamma)_{nf}}{(\rho\gamma)_f}\ ,\ Re=\frac{\rho_b cd}{\mu_b}\ ,\ \bar{\psi}=\frac{\psi}{cd}\ ,\ G_r=\frac{\rho_b g\gamma_b d^2 T_0}{\mu_b c}\ ,$$
$$E_c=\frac{c^2}{c_p\bar{T}_0}\ ,\ M^2=\frac{\sigma B_0^2 d^2}{\mu_b}\ ,\ \bar{\varphi}=\frac{k_B\hat{T}\varphi}{ez}\ ,\ U=\frac{\epsilon_0 k_b\hat{T}E_x}{ez\mu_b c}\ ,\ k=\sqrt{\frac{2n_0 e^2 z^2 d^2}{\epsilon_0 k_B\hat{T}}}\ ,\ B_r=E_c P_r\ ,\ R_d=$$
$$\frac{16\sigma^*}{3k^*\mu_b c_p}\bar{T}_0^3 \quad (8)$$

This problem can be simplified to a notable extent by introducing stream function as:

$$u=\frac{\partial \psi}{\partial y}\ \ ,\ \ v=-\delta\frac{\partial \psi}{\partial x} \quad (9)$$

From the above Eqns. with $\ll 1$, $Re \ll 1$ we have:

$$\frac{\partial p}{\partial x}=\frac{1}{(1-\Phi)^{2.5}}\frac{\partial^3 \psi}{\partial y^3}-M^2\left(\frac{\partial \psi}{\partial y}+1\right)-\frac{1}{D_a(1-\Phi)^{2.5}}\left(\frac{\partial \psi}{\partial y}+1\right)+U\left(\frac{\partial^3 \varphi}{\partial y^3}\right)+G_r L\theta \quad (10)$$

where $D_a=\frac{k}{d^2}$. And by the derivative of Eq. (10) we obtain:

$$0=\frac{1}{(1-\Phi)^{2.5}}\frac{\partial^4 \psi}{\partial y^4}-M^2\frac{\partial^2 \psi}{\partial y^2}-\frac{1}{D_a(1-\Phi)^{2.5}}\frac{\partial^2 \psi}{\partial y^2}+U\frac{\partial^3 \varphi}{\partial y^3}+G_r L\frac{\partial \theta}{\partial y} \quad (11)$$

$$(A+R_d P_r)\frac{\partial^2 \theta}{\partial y^2}+\frac{B_r}{(1-\Phi)^{2.5}}\left(\frac{\partial^2 \psi}{\partial y^2}\right)^2=0 \quad (12)$$

4. Shear Stress

The term $\tau \cdot L^T$ can be computed from the definition of Dot product of two tensor and the constitutive equations can be defined as [16]:

$$\tau=-\bar{P}I+\bar{\tau}$$
$$\bar{\tau}=2\mu_b e_{ij} \quad (13)$$

$$e_{ij}=\frac{1}{2}\left(\frac{\partial u_i}{\partial x_j}+\frac{\partial u_j}{\partial x_i}\right) \quad (14)$$

And when normalize the resulting equation by using the dimensionless quantities with stream function equation and $\ll 1$, $Re \ll 1$ we get:

$$\tau_{xx}=0\ ,\ \tau_{yy}=0\ ,\ \text{and}\ \tau_{xy}=\tau_{yx}=\frac{\partial^2 \psi}{\partial y^2} \quad (15)$$

5. Rate of Volume Flow and Boundary Conditions

The dimensional volume flow rate in the fixed frame reference $(\bar{x}\ ,\bar{y})$ is given as [17]:

$$Q(\bar{x}\ ,\bar{t})=\int_{\bar{H}_2(\bar{x}\ ,\bar{t})}^{\bar{H}_1(\bar{x}\ ,\bar{t})} U(\bar{x}\ ,\bar{y}\ \ ,\bar{t})\ d\bar{y} \quad (16)$$

where $\bar{H}_1$, $\bar{H}_2$ are functions of $\bar{x}$ and $\bar{t}$, the dimensional volume flow rate in the wave frame be steady and defined as:

$$q = \int_{\bar{H}_2(\bar{x})}^{\bar{H}_1(\bar{x})} U(\bar{x}, \bar{y})\, d\bar{y} \tag{17}$$

Substituting Eq. (17) in Eq. (16) we have:

$$Q = q + c\bar{H}_1 - c\bar{H}_2 \tag{18}$$

The definition of time averaged flow over a period $T = \lambda/c$ at a fixed position $\bar{x}$ of the peristaltic wave is:

$$\bar{Q} = \frac{1}{T}\int_0^T Q\, d\bar{t} \tag{19}$$

By substituting Eq. (18) in Eq. (19) with integration, we get:

$$\bar{Q} = q + a_1 c \sin\left[\frac{2\pi}{\lambda}(\bar{X} - c\bar{t})\right] + a_2 c \sin\left[\frac{2\pi}{\lambda}(\bar{X} - c\bar{t}) + \Phi\right] \tag{20}$$

Thus, $F = \bar{Q}/cd$ and $\theta = q/cd$. However, Eq. (20) can be written as:

$$F(x, t) = \theta + a\sin[2\pi(x - t)] + b\sin[2\pi(x - t) + \Phi] \tag{21}$$

$$F = \int_{h_2(x)}^{h_1(x)} \frac{\partial\psi}{\partial y} dy = \psi\big(h_1(x)\big) - \psi\big(h_2(x)\big) \tag{22}$$

where, $\psi\big(h_1(x)\big) = \frac{F}{2}$ and $\psi\big(h_2(x)\big) = -\frac{F}{2}$ the boundary conditions dimensionless stream function will take the following form:

$$\psi = \frac{F}{2} \quad , \quad \frac{\partial\psi}{\partial y} = 0 \quad at\ y = h_1 \quad and \quad \psi = -\frac{F}{2} \quad , \quad \frac{\partial\psi}{\partial y} = 0 \quad at\ y = h_2 \tag{23}$$

In which, $h_1 = 1 + a\sin\big(2\pi(x - t)\big)$ and $h_2 = -1 - b\sin(2\pi(x - t) + \Phi)$.

6. Pressure Rise Rate

The non-dimensional form of ΔP "The average rise in pressure per wave length" can be given as:

$$\Delta P = \left(\int_0^1\int_0^1 \frac{\partial P}{\partial x}\, dxdt\right)_{y=0} \tag{24}$$

$$\frac{\partial p}{\partial x} = \frac{1}{(1-\Phi)^{2.5}}\frac{\partial^3\psi}{\partial y^3} - \left(M^2 + \frac{1}{D_a(1-\Phi)^{2.5}}\right)\left(\frac{\partial\psi}{\partial y} + 1\right) + Uk^2\frac{\cosh(ky)}{\cosh(kh)} + G_r L\theta \tag{25}$$

Simplifying Eq. (25) as follows by differentiating both sides with respect to y.

$$\frac{1}{(1-\Phi)^{2.5}}\frac{\partial^4\psi}{\partial y^4} - \left(M^2 + \frac{1}{D_a(1-\Phi)^{2.5}}\right)\frac{\partial^2\psi}{\partial y^2} + Uk^3\frac{\sinh(ky)}{\cosh(kh)} + G_r L\frac{\partial\theta}{\partial y} = 0 \tag{26}$$

Or

$$(A + P_r R_d)\frac{\partial^2\theta}{\partial y^2} + \frac{B_r}{(1-\Phi)^{2.5}}\left(\frac{\partial^2\psi}{\partial y^2}\right)^2 = 0 \tag{27}$$

Where, the slip boundary conditions are:

$$\psi = 0 \quad , \quad \frac{\partial^2\psi}{\partial y^2} = 0 \quad at\ y = h_1 \tag{28}$$

$$\psi = F \quad , \quad \frac{\partial\psi}{\partial y} = -1 - \frac{\gamma}{(1-\Phi)^{2.5}}\frac{\partial^2\psi}{\partial y^2} \quad at\ y = h_1 = 1 + \epsilon\sin(2\pi x) \tag{29}$$

$$\frac{\partial\theta}{\partial y} = 0 \quad at\ y = h_1 \quad , \quad \theta + \mu\frac{\partial\theta}{\partial y} = 0 \quad at\ y = h_2 \tag{30}$$

where μ and γ are presented the dimensionless velocity the slip parameter and thermal the slip parameter. The results of Eqs. (25 – 30) having a high order non-linear partial differential. So, it is difficult to solve as exact solution founded.

7. Method of Solution

$$\begin{aligned} \psi &= \psi_0 + B_r\psi_1 \\ P &= P_0 + B_r P_1 \\ \theta &= \theta_0 + B_r\theta_1 \end{aligned} \tag{31}$$

Now, substituting Eq. (31) into Eqs. (25 – 30) and equating the coefficients of equal power of Brinkmann number, getting zero and first order system.

7.1 Zeroth Order System $\left(B_r^{(0)}\right)$ *with it's Boundary Conditions*

The corresponding zeroth order system are:

$$\frac{\partial P_0}{\partial x} = \frac{1}{(1-\Phi)^{2.5}}\frac{\partial^3\psi_0}{\partial y^3} - M^2\frac{\partial\psi_0}{\partial y} - \frac{1}{D_a(1-\Phi)^{2.5}}\frac{\partial\psi_0}{\partial y} + Uk^2\frac{\cosh(ky)}{\cosh(kh)} + G_rL\theta_0 \tag{32}$$

$$\frac{1}{(1-\Phi)^{2.5}}\frac{\partial^4\psi_0}{\partial y^4} - \left(M^2 + \frac{1}{D_a(1-\Phi)^{2.5}}\right)\frac{\partial^2\psi_0}{\partial y^2} + Uk^3\frac{\sinh(ky)}{\cosh(kh)} + G_rL\frac{\partial\theta_0}{\partial y} = 0 \tag{33}$$

$$(A + R_dP_r)\frac{\partial^2\theta_0}{\partial y^2} = 0 \tag{34}$$

With the boundary conditions:

$$\begin{aligned} &\psi_0 = F \quad , \quad \frac{\partial\psi_0}{\partial y} = -1 - \frac{\gamma}{(1-\Phi)^{2.5}}\frac{\partial^2\psi_0}{\partial y^2} \quad at\ y = h_1 = 1 + \epsilon\sin(2\pi x) \\ &\psi_0 = 0 \quad , \quad \frac{\partial^2\psi_0}{\partial y^2} = 0 \quad at\ y = h_2 \\ &\frac{\partial\theta_0}{\partial y} = 0 \quad at\ y = h_2 \quad , \quad \theta_0 + \mu\frac{\partial\theta_0}{\partial y} = 0 \quad at\ y = h_1 \end{aligned} \tag{35}$$

7.2 First Order System $\left(B_r^{(1)}\right)$ *with Boundary Conditions*

$$\frac{\partial P_1}{\partial x} = \frac{1}{(1-\Phi)^{2.5}}\frac{\partial^3\psi_1}{\partial y^3} - \left(M^2\frac{\partial\psi_0}{\partial y} + \frac{1}{D_a(1-\Phi)^{2.5}}\right)\frac{\partial\psi_1}{\partial y} + G_rL\theta_1 \tag{36}$$

$$\frac{1}{(1-\Phi)^{2.5}}\frac{\partial^4\psi_1}{\partial y^4} - \left(M^2 + \frac{1}{D_a(1-\Phi)^{2.5}}\right)\frac{\partial^2\psi_1}{\partial y^2} + G_rL\frac{\partial\theta_1}{\partial y} = 0 \tag{37}$$

$$(A + R_dP_r)\frac{\partial^2\theta_1}{\partial y^2} + \frac{1}{(1-\Phi)^{2.5}}\left(\frac{\partial^2\psi_0}{\partial y^2}\right)^2 = 0 \tag{38}$$

With the boundary conditions:

$$\begin{aligned} &\psi_1 = 0 \quad , \quad \frac{\partial\psi_1}{\partial y} = -\frac{\gamma}{(1-\Phi)^{2.5}}\frac{\partial^2\psi_1}{\partial y^2} \quad at\ y = h_1 = 1 + \epsilon\sin(2\pi x) \\ &\psi_1 = 0 \quad , \quad \frac{\partial^2\psi_1}{\partial y^2} = 0 \quad at\ y = h_2 \\ &\frac{\partial\theta_1}{\partial y} = 0 \quad at\ y = h_2 \quad , \quad \theta_1 + \mu\frac{\partial\theta_1}{\partial y} = 0 \quad at\ y = h_1 \end{aligned} \tag{39}$$

By using MATHEMATICA software, zeroth and first order systems are solved for an exact solution and resulting for stream function, pressure gradient and temperature distribution.

8 The Solution of Systems

8.1 Zeroth Order System

We found that the solution of Eqs.(33-34) under the associated boundary conditions in Eq. (35) given as:

$$\psi_0[y] = \mathrm{c3} + y\mathrm{c4} + \frac{\mathrm{c2Gr}Ly^2}{2(\mathrm{A2}+M^2)} - \frac{\mathrm{A1}(-\mathrm{e}^{\frac{\sqrt{\mathrm{A2}+M^2}y}{\sqrt{\mathrm{A1}}}}\mathrm{c1} - \mathrm{e}^{-\frac{\sqrt{\mathrm{A2}+M^2}y}{\sqrt{\mathrm{A1}}}}\mathrm{c2})}{\mathrm{A2}+M^2} + \frac{\mathrm{A3Sech[h1}k\mathrm{]Sinh}[ky]}{k^2(\mathrm{A2}-\mathrm{A1}k^2+M^2)}$$

$$\theta_0[y] = c_1 + yc_2$$

where c_i, $\mathrm{i} = 1, 2, 3, 4, 5, 6, 7, 8, 9, 10, 11, \& 12$ are constants can be obtained by using the boundary conditions in Eq. (35).

8.2 First Order System

By solving Eqs. (36-38) with the associated boundary conditions in Eq. (39), we get:

$$\begin{aligned}\psi_1[y] = \mathrm{c9} + y\mathrm{c10} - ((&3\mathrm{A1A3}^2\mathrm{Gr}L(\mathrm{A2}+M^2)^{7/2}(\mathrm{A2}-\mathrm{A1}k^2+M^2)^3(4\mathrm{A2}-\mathrm{A1}k^2\\&+4M^2)\mathrm{Cosh}[2ky](\mathrm{Cosh[h1}k] + \mathrm{Sinh[h1}k])^2 + \cdots)\\&- \cdots\cdots\cdots\cdots/(24k^3(\mathrm{A2}+M^2)^{7/2}(\mathrm{A2}-\mathrm{A1}k^2+M^2)^4(-2\sqrt{\mathrm{A1}}k + \sqrt{(\mathrm{A2}\\&+M^2)})(-\sqrt{\mathrm{A1}}k + \sqrt{(\mathrm{A2}+M^2)})(\sqrt{\mathrm{A1}}k + \sqrt{(\mathrm{A2}+M^2)})(2\sqrt{\mathrm{A1}}k + \sqrt{(\mathrm{A2}\\&+M^2)})(-\sqrt{\mathrm{A1}}k + 2\sqrt{(\mathrm{A2}+M^2)})(\sqrt{\mathrm{A1}}k + 2\sqrt{(\mathrm{A2}+M^2)})(A\\&+\mathrm{PrRd})(1+\mathrm{Cosh[2h1}k] + \mathrm{Sinh[2h1}k])^2))\end{aligned}$$

$$\begin{aligned}\theta_1[y] = \mathrm{c7} + y\mathrm{c8} - (\mathrm{A1}(&\frac{1}{\mathrm{A2}+M^2}2\mathrm{A1e}^{\frac{\sqrt{\mathrm{A2}+M^2}y}{\sqrt{\mathrm{A1}}}}(\mathrm{A2}^3\mathrm{c2c3Gr}L - 2\mathrm{A1A2}^2\mathrm{c2c3Gr}k^2L\\&+\mathrm{A1}^2\mathrm{A2c2c3Gr}k^4L + 3\mathrm{A2}^2\mathrm{c2c3Gr}LM^2 - 4\mathrm{A1A2c2c3Gr}k^2LM^2\\&+\mathrm{A1}^2\mathrm{c2c3Gr}k^4LM^2 + 3\mathrm{A2c2c3Gr}LM^4 - 2\mathrm{A1c2c3Gr}k^2LM^4 + \mathrm{c2c3Gr}LM^6)\\&+\cdots - \cdots\cdots\cdots\cdots))/((\mathrm{A2}+M^2)^2(\mathrm{A2}-\mathrm{A1}k^2+M^2)^2(A+\mathrm{PrRd}))\end{aligned}$$

where c_i, $\mathrm{i} = 1, 2, 3, 4, 5, 6, 7, 8, 9, 10, 11, \& 12$ are constants can be determined by using the boundary conditions in Eq. (39) and software of "MATHEMATICA" program.

8.3 Solution of the Pressure Gradient

The pressure gradient defined as:

$$\Delta P = \left(\int_0^1 \int_0^1 \frac{\partial P}{\partial x}\, dx\, dt\right)_{y=0}$$

This integration was evaluating by using the "MATHEMATICA" software and the obtained results were by the perturbation method that used for the analytical solution.

$$P_0[x] = -\frac{k(\mathrm{A2c6} + \mathrm{c6}M^2 + \mathrm{c2Gr}Ly) + (\mathrm{A3} - k^3U)\mathrm{Cosh}[ky]\mathrm{Sech[h1}k]}{k} + \mathrm{Gr}L\theta_0$$

$$\begin{aligned}P_1[x] = (&6\mathrm{A1A3}^2\mathrm{Gr}kL(\mathrm{A2}+M^2)(\mathrm{A2}-\mathrm{A1}k^2+M^2)^3(4\mathrm{A2}-\mathrm{A1}k^2\\&+4M^2)\mathrm{Cosh}[2ky](\mathrm{Cosh[h1}k] + \mathrm{Sinh[h1}k])^2\\&+\frac{1}{(\mathrm{A2}+M^2)^2}24\mathrm{A1Gr}k^3L(\mathrm{A2}-\mathrm{A1}k^2+M^2)^3\cdots - \cdots\cdots\cdots\cdots\\&+\frac{\mathrm{A3}^2(\mathrm{A2}+M^2)^2\mathrm{Sech[h1}k]^2(\mathrm{Cosh}[2ky] - \mathrm{Sinh}[2ky])}{k^2}\\&+\frac{\mathrm{A3}^2(\mathrm{A2}+M^2)^2\mathrm{Sech[h1}k]^2\mathrm{Sinh}[2ky]}{k^2}))\end{aligned}$$

9. Results and Discussions

The numerical and computational results are discussed for the problem of electroosmosis augmented MHD peristaltic transport of SWCNTs suspension in a porous media of an incompressible non-Newtonian fluid under the effect of normal magnetic field through porous media in a symmetric channel with no-slip conditions.

9.1 Temperature Profile

The temperature profile are sketched for two dimensional channel upon the variation of important parameters involved in the expression of temperature profile via Figures 2.a – 2.l with different parameters Darcy number (D_a), varies in the range (Φ), Helmholtz-Smoluchowski (U), coefficient of thermal expansion (γ), amplitudes wave $(a\,, b)$, viscosity (μ), Grashoof number (G_r), flow rate (F), Prandtl number (P_r), Brinkman number (B_r), and radiation parameter (R_d).

Figure 2.a shows that the increasing value of (D_a) with increasing of temperature, it is balance at the middle of channel but for increasing of channel width, the temperature continuous to low at near the walls. From Figure 2.b, the resulting graph displays growth in temperature as (Φ) decreases. Figure 2.c, illustrates increase function for temperature distribution with increasing values of (U) as well as a stable for (θ) is noticed in the central part of the channel, the temperature generated by the acceleration of ionic species due to electroosmotic forces and it can be seen through resulting sketch that temperature is maximum for $(U=-2)$ whereas minimum for $(U=2)$. This behaviour can be justified by $(U=-2)$ means electric field in direction of peristaltic pumping, $(U=0)$ means there is no electric field and $(U=2)$ corresponds to opposing electric body forces. The effect of (U) is appeared when decreases the parameter (Φ). Figure 2.d, decreasing value of (γ) implies that increasing value of temperature. The influence of upper wall amplitude (a) on temperature profile is sketched in Figure 2.e. We noticed that the temperature arising with ascending values of (a). The temperature for the amplitude (b) of lower wall is shown in Figure 2.f. It has been observed that an increase in (b) values causes as increase in the magnitude of temperature at the lower wall and center part of asymmetric channel. The impact of (μ) on the temperature profile is shown in Figure 2.g. It is found that the temperature increases when (μ) increases. Whereas the heat transfer phenomenon is appear clearly in Figure 2.h, the effect of (G_r) was discussed, which that increasing value leads to increasing of the parameter and the value of temperature is highest at the centre of channel. It can examine from Figure 2.i, the behaviour of the temperature with (F), it was observed that (θ) decreases with increasing values of (F). Figure 2.j, Prandtl number (P_r) not effect in temperature and the profile is parabolic increasing at the centre of channel mostly. Figure 2.k increasing values of (B_r) leads to increase the temperature. This confirms the fact "viscous dissipation effects with increase the temperature". The change value of (R_d) in Figure 2.l by increasing leads to decreasing the value of temperature.

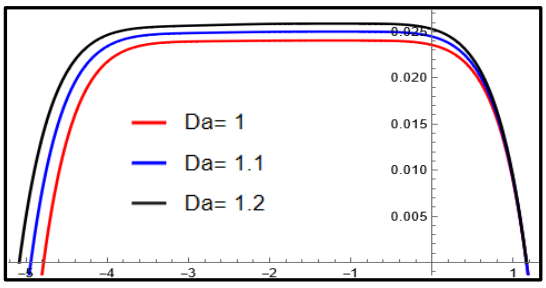

Figure 2.a: Variation of temperature as a function versus y-direction with different parameters $[D_a = 1, 1.1\ and\ 1.2,\ \phi = \frac{\pi}{4},\ k = 0.2,\ U = 0.2,\ \gamma = 0.2,\ a = 0.4,\ b = 0.2,\ \mu = 0.2,\ M = 0.7,\ G_r = 6,\ F = 1,\ P_r = 6.1,\ B_r = 0.3,\ R_d = 1.5,\ L = 0.2,\ A = 0.1,$ and x=1].

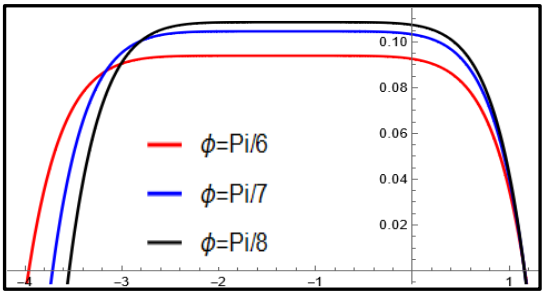

Figure 2.b: Variation of temperature as a function versus y-direction with different parameters $[D_a = 1,\ \phi = \frac{\pi}{6}, \frac{\pi}{7}\ and\ \frac{\pi}{8},\ k = 0.2,\ U = 0.2,\ \gamma = 0.2,\ a = 0.4,\ b = 0.2,\ \mu = 0.2,\ M = 0.7,\ G_r = 6,\ F = 1,\ P_r = 6.1,\ B_r = 0.3,\ R_d = 1.5,\ L = 0.2,\ A = 0.1,$ and x=1].

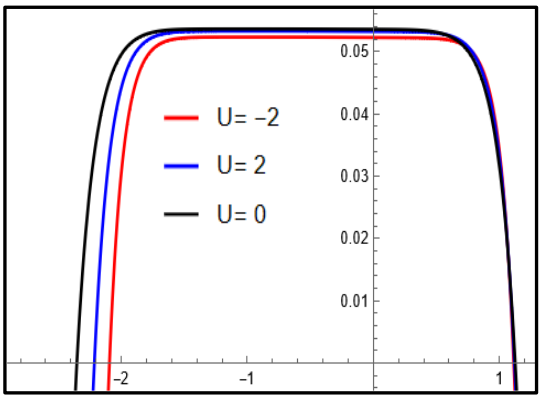

Figure 2.c: Variation of temperature as a function versus y-direction with different parameters [$D_a = 1$, $\phi = 0.1, 0.2\ and\ 0.3$, $k = 0.2$, $U = -2, 2\ and\ 0$, $\gamma = 0.2$, $a = 0.4$, $b = 0.2$, $\mu = 0.2$, $M = 5$, $G_r = 6$, $F = 1$, $P_r = 6.1$, $B_r = 0.3$, $R_d = 1.5$, $L = 0.2$, $A = 0.1$, and x=1].

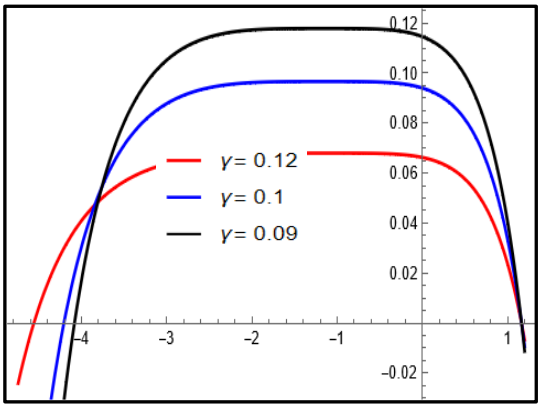

Figure 2.d: Variation of temperature as a function versus y-direction with different parameters [$D_a = 1$, $\phi = \frac{\pi}{4}$, $k = 0.2$, $U = 0.2$, $\gamma = 0.12, 0.1\ and\ 0.09$, $a = 0.4$, $b = 0.2$, $\mu = 0.2$, $M = 0.7$, $G_r = 6$, $F = 1$, $P_r = 6.1$, $B_r = 0.3$, $R_d = 1.5$, $L = 0.2$, $A = 0.1$, and x=1].

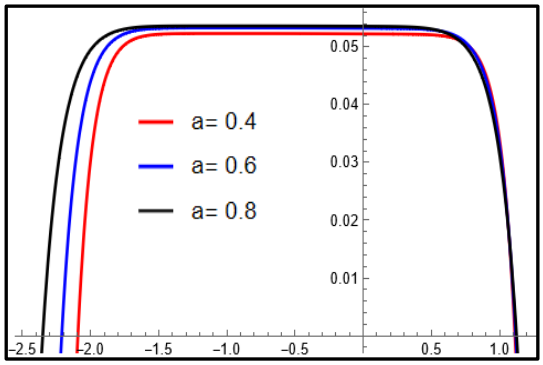

Figure 2.e: Variation of temperature as a function versus y-direction with different parameters [$D_a = 1$, $\phi = 0.1, 0.2\ and\ 0.3$, $k = 0.2$, $U = -2$, $\gamma = 0.2$, $a = 0.4, 0.6\ and\ 0.8$, $b = 0.2$, $\mu = 0.2$, $M = 5$, $\square_r = 6$, $F = 1$, $P_r = 6.1$, $B_r = 0.3$, $R_d = 1.5$, $L = 0.2$, $A = 0.1$, and x=1].

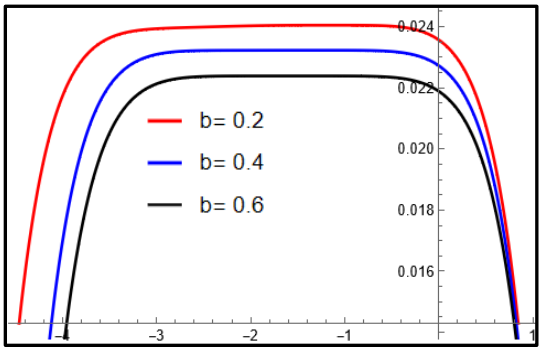

Figure 2.f: Variation of temperature as a function versus y-direction with different parameters [$D_a = 1$, $\phi = \frac{\pi}{4}$, $k = 0.2$, $U = 0.2$, $\gamma = 0.2$, $a = 0.4$, $b = 0.2, 0.4\ and\ 0.6$, $\mu = 0.2$, $M = 0.7$, $G_r = 6$, $F = 1$, $P_r = 6.1$, $B_r = 0.3$, $R_d = 1.5$, $L = 0.2$, $A = 0.1$, and x=1].

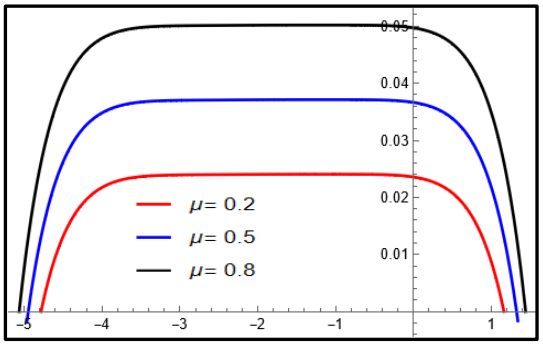

Figure 2.g: Variation of temperature as a function versus y-direction with different parameters [$D_a = 1$, $\phi = \frac{\pi}{4}$, $k = 0.2$, $U = 0.2$, $\gamma = 0.2$, $a = 0.4$, $b = 0.2$, $\mu = 0.2, 0.5\ and\ 0.8$, $M = 0.7$, $G_r = 6$, $F = 1$, $P_r = 6.1$, $B_r = 0.3$, $R_d = 1.5$, $L = 0.2$, $A = 0.1$, and x=1].

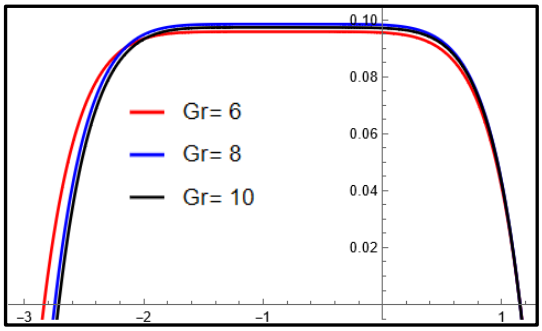

Figure 2.h: Variation of temperature as a function versus y-direction with different parameters [$D_a = 1$, $\phi = 0.1, 0.2\ and\ 0.3$, $k = 0.2$, $U = 0.2$, $\gamma = 0.2$, $a = 0.4$, $b = 0.2$, $\mu = 0.2$, $M = 0.7$, $G_r = 6, 8\ and\ 10$, $F = 1$, $P_r = 6.1$, $B_r = 0.3$, $R_d = 1.5$, $L = 0.2$, $A = 0.1$, and x=1].

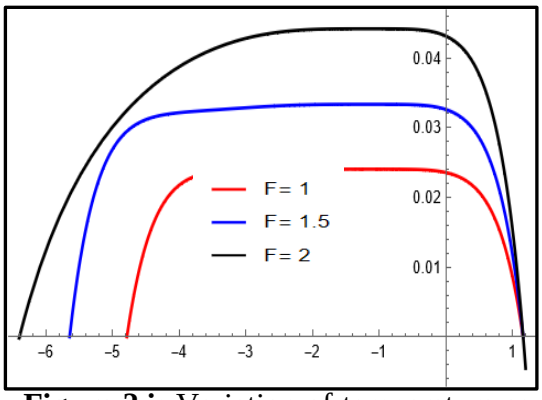

Figure 2.i: Variation of temperature as a function versus y-direction with different parameters [$D_a = 1$, $\phi = \frac{\pi}{4}$, $k = 0.2$, $U = 0.2$, $\gamma = 0.2$, $a = 0.4$, $b = 0.2$, $\mu = 0.2$, $M = 0.7$, $G_r = 6$, $F = 1, 1.5\ and\ 2$, $P_r = 6.1$, $B_r = 0.3$, $R_d = 1.5$, $L = 0.2$, $A = 0.1$, and x=1].

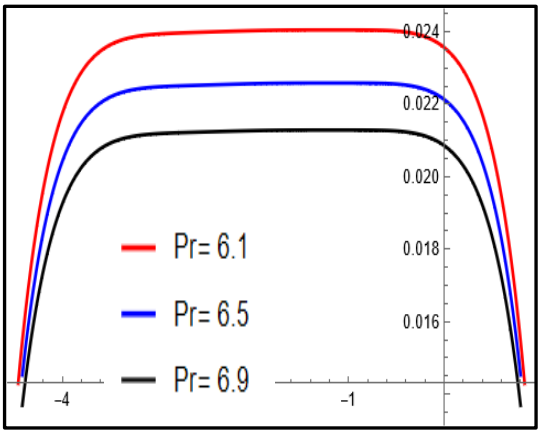

Figure 2.j: Variation of temperature as a function versus y-direction with different parameters [$D_a = 1$, $\phi = \frac{\pi}{4}$, $k = 0.2$, $U = 0.2$, $\gamma = 0.2$, $a = 0.4$, $b = 0.2$, $\mu = 0.2$, $M = 0.7$, $G_r = 6$, $F = 1$, $P_r = 6.1, 6.5\ and\ 6.9$, $B_r = 0.3$, $R_d = 1.5$, $L = 0.2$, $A = 0.1$, and x=1].

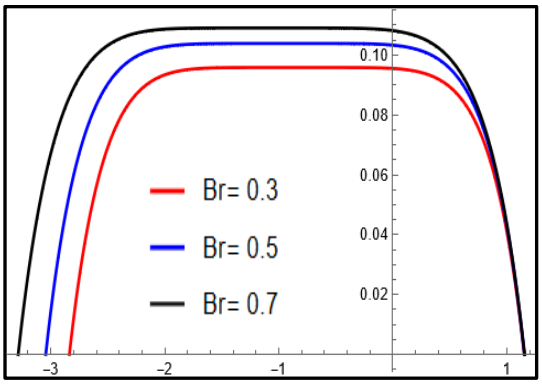

Figure 2.k: Variation of temperature as a function versus y-direction with different parameters [$D_a = 1$, $\phi = 0.1, 0.2\ and\ 0.3$, $k = 0.2$, $U = 0.2$, $\gamma = 0.2$, $a = 0.4$, $b = 0.2$, $\mu = 0.2$, $M = 0.7$, $G_r = 6$, $F = 1$, $P_r = 6.1$, $B_r = 0.3, 0.5\ and\ 0.7$, $R_d = 1.5$, $L = 0.2$, $A = 0.1$, and x=1].

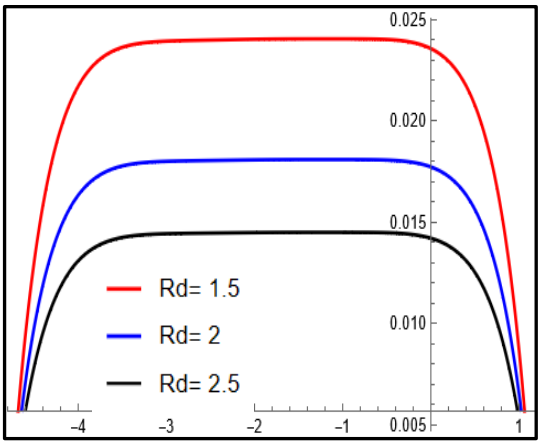

Figure 2.l: Variation of temperature as a function versus y-direction with different parameters [$D_a = 1$, $\phi = \frac{\pi}{4}$, $k = 0.2$, $U = 0.2$, $\gamma = 0.2$, $a = 0.4$, $b = 0.2$, $\mu = 0.2$, $M = 0.7$, $G_r = 6$, $F = 1$, $P_r = 6.1$, $B_r = 0.3$, $R_d = 1.5, 2\ and\ 2.5$, $L = 0.2$, $A = 0.1$, and x=1].

Figure 2: Variation of temperature as a function versus y-direction with different parameters [D_a, Φ, U, γ, a, b, μ, G_r, F, P_r, B_r, R_d, and x=1].

9.2 Trapping Formulation

A fascinating phenomenon happens in the peristaltic flows where the closed stream lines entice the quantity of fluid normally named as bolus "trapping phenomenon" internal the channel closed to the walls and this trapping bolus moves inside the course of the wave engendering "or propagation". The behaviour of stream function is illustrated in Figures 3.a – 3.aj, via Figures 3.a,b,c it can be seen that when (Φ) increments at that point, the estimate of bolus will be decrease. It delineates from Figures 3.d,e,f that if (U) enhanced the measure of bolus increases gradually. Observing the behaviour from magnetic parameter (U). Figures 3.g,h,i show that there is an increasing on trapping when (D_a) increases. Figures 3.j,k,l show that as (a) increases the bolus increases. Figures 3.m,n,o show that as (b) increase, the measure of bolus rise to tend. Figures 3.p,q,r, increasing values of (G_r) bolus' size rise to tend. Increasing values of (P_r), the bolus getting bigger, see Figures 3.s,t,u. When (R_d) values increases the bolus decreases as in Figures 3.v,w,x. In Figures 3.y,z,aa, the number of boluses increasing. (B_r) in these Figures, it is observed that the trapped boluses are begin to increases when these values increasing; whereas begin to be appear when increasing values of $(F\&\gamma)$ in Figures 3.ab,ac,ad and Figures 3.ae,af,ag lead to expand of the wave and turn into winding waves. It is clear from Figures 3.ah,ai,aj that the trapped bolus are decay when the value of (μ) increasing.

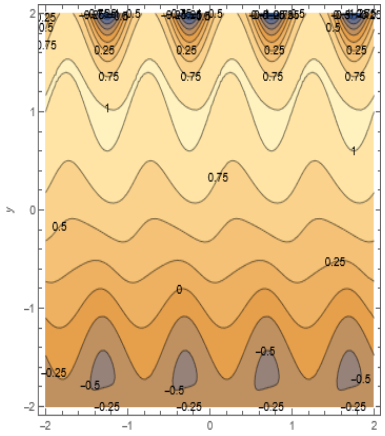

Figure 3.a: Influence of different parameters on stream function [$D_a = 1$, $\phi = \frac{\pi}{6}$, $U = 2$, $\gamma = 0.2$, $a = 0.4$, $b = 0.2$, $\mu = 0.2$, $G_r = 6$, $F = 1$, $P_r = 6.1$, $B_r = 0.3$, $R_d = 1.5$, $x = -2\ to\ 2$, and $y = -2\ to\ 2$].

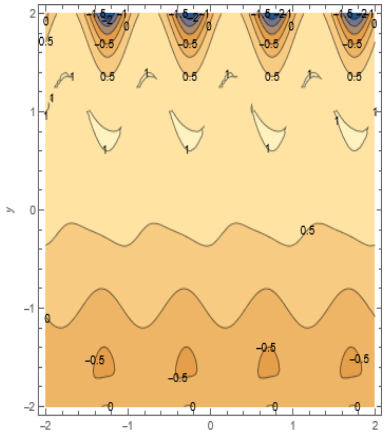

Figure 3.b: Influence of different parameters on stream function [$D_a = 1$, $\phi = \frac{\pi}{7}$, $U = 2$, $\gamma = 0.2$, $a = 0.4$, $b = 0.2$, $\mu = 0.2$, $G_r = 6$, $F = 1$, $P_r = 6.1$, $B_r = 0.3$, $R_d = 1.5$, $x = -2\ to\ 2$, and $y = -2\ to\ 2$].

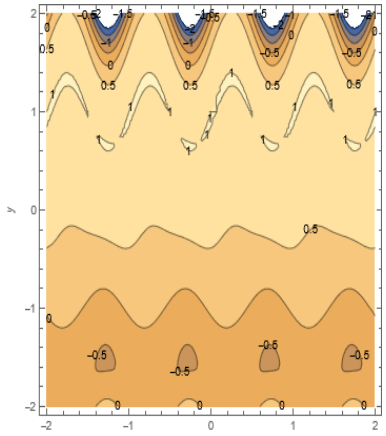

Figure 3.c: Influence of different parameters on stream function [$D_a = 1$, $\phi = \frac{\pi}{8}$, $U = 2$, $\gamma = 0.2$, $a = 0.4$, $b = 0.2$, $\mu = 0.2$, $G_r = 6$, $F = 1$, $P_r = 6.1$, $B_r = 0.3$, $R_d = 1.5$, $x = -2\ to\ 2$, and $y = -2\ to\ 2$].

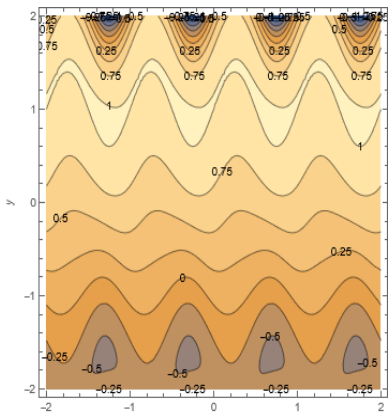

Figure 3.g: Influence of different parameters on stream function [$D_a = 1$, $\phi = \frac{\pi}{6}$, $U = 2$, $\gamma = 0.2$, $a = 0.4$, $b = 0.2$, $\mu = 0.2$, $G_r = 6$, $F = 1$, $P_r = 6.1$, $B_r = 0.3$, $R_d = 1.5$, $x = -2\ to\ 2$, and $y = -2\ to\ 2$].

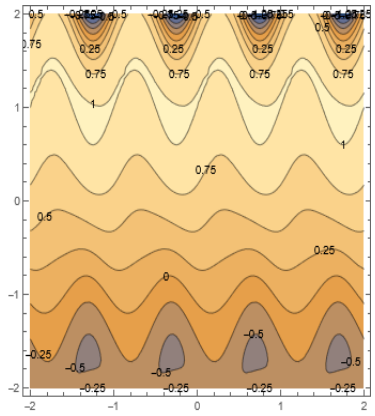

Figure 3.h: Influence of different parameters on stream function [$D_a = 1.1$, $\phi = \frac{\pi}{6}$, $U = 2$, $\gamma = 0.2$, $a = 0.4$, $b = 0.2$, $\mu = 0.2$, $G_r = 6$, $F = 1$, $P_r = 6.1$, $B_r = 0.3$, $R_d = 1.5$, $x = -2\ to\ 2$, and $y = -2\ to\ 2$].

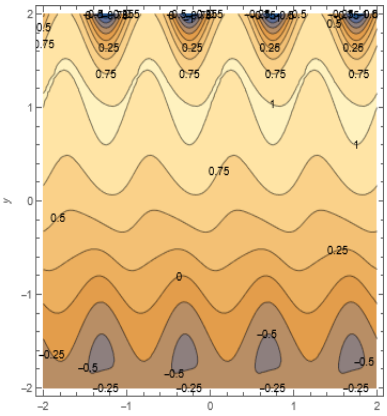

Figure 3.i: Influence of different parameters on stream function [$D_a = 1.2$, $\phi = \frac{\pi}{6}$, $U = 2$, $\gamma = 0.2$, $a = 0.4$, $b = 0.2$, $\mu = 0.2$, $G_r = 6$, $F = 1$, $P_r = 6.1$, $B_r = 0.3$, $R_d = 1.5$, $x = -2\ to\ 2$, and $y = -2\ to\ 2$].

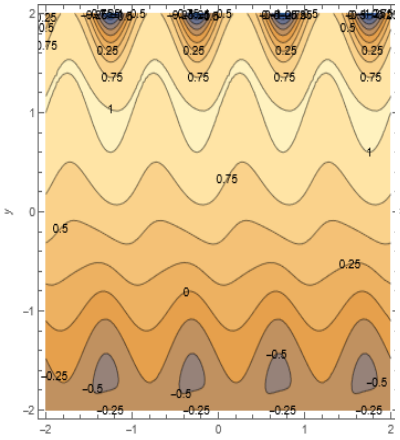

Figure 3.j: Influence of different parameters on stream function [$D_a = 1$, $\phi = \frac{\pi}{6}$, $U = 2$, $\gamma = 0.2$, $a = 0.4$, $b = 0.2$, $\mu = 0.2$, $G_r = 6$, $F = 1$, $P_r = 6.1$, $B_r = 0.3$, $R_d = 1.5$, $x = -2\ to\ 2$, and $y = -2\ to\ 2$].

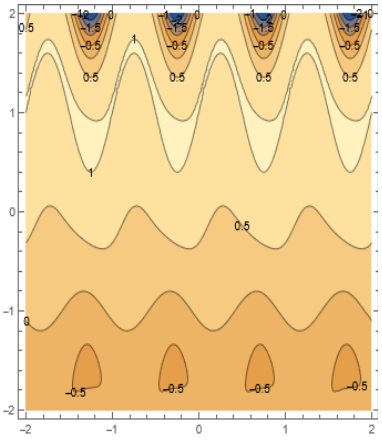

Figure 3.k: Influence of different parameters on stream function [$D_a = 1$, $\phi = \frac{\pi}{6}$, $U = 2$, $\gamma = 0.2$, $a = 0.6$, $b = 0.2$, $\mu = 0.2$, $G_r = 6$, $F = 1$, $P_r = 6.1$, $B_r = 0.3$, $R_d = 1.5$, $x = -2\ to\ 2$, and $y = -2\ to\ 2$].

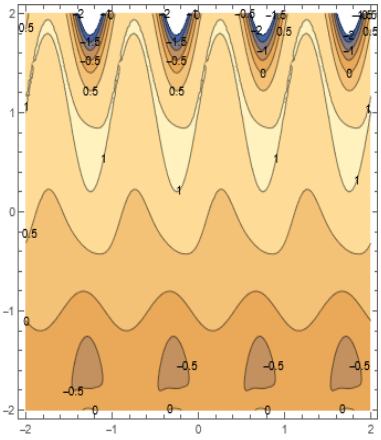

Figure 3.l: Influence of different parameters on stream function [$D_a = 1$, $\phi = \frac{\pi}{6}$, $U = 2$, $\gamma = 0.2$, $a = 0.8$, $b = 0.2$, $\mu = 0.2$, $G_r = 6$, $F = 1$, $P_r = 6.1$, $B_r = 0.3$, $R_d = 1.5$, $x = -2\ to\ 2$, and $y = -2\ to\ 2$].

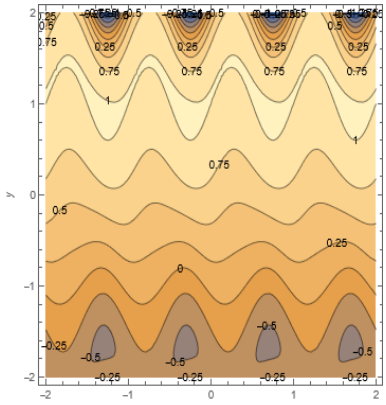

Figure 3.m: Influence of different parameters on stream function [$D_a = 1$, $\phi = \frac{\pi}{6}$, $U = 2$, $\gamma = 0.2$, $a = 0.4$, $b = 0.2$, $\mu = 0.2$, $G_r = 6$, $F = 1$, $P_r = 6.1$, $B_r = 0.3$, $R_d = 1.5$, $x = -2\ to\ 2$, and $y = -2\ to\ 2$].

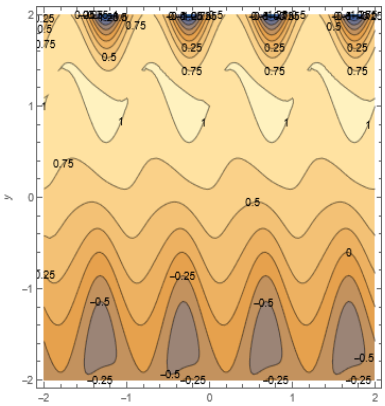

Figure 3.n: Influence of different parameters on stream function [$D_a = 1$, $\phi = \frac{\pi}{6}$, $U = 2$, $\gamma = 0.2$, $a = 0.4$, $b = 0.4$, $\mu = 0.2$, $G_r = 6$, $F = 1$, $P_r = 6.1$, $B_r = 0.3$, $R_d = 1.5$, $x = -2\ to\ 2$, and $y = -2\ to\ 2$].

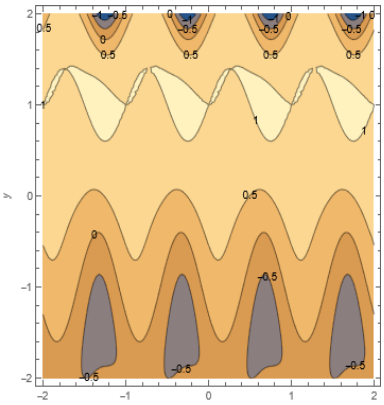

Figure 3.o: Influence of different parameters on stream function [$D_a = 1$, $\phi = \frac{\pi}{6}$, $U = 2$, $\gamma = 0.2$, $a = 0.4$, $b = 0.6$, $\mu = 0.2$, $G_r = 6$, $F = 1$, $P_r = 6.1$, $B_r = 0.3$, $R_d = 1.5$, $x = -2\ to\ 2$, and $y = -2\ to\ 2$].

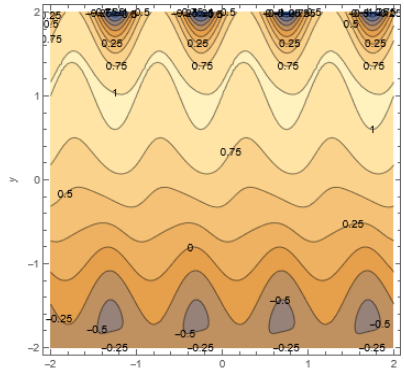

Figure 3.p: Influence of different parameters on stream function [$D_a = 1$, $\phi = \frac{\pi}{6}$, $U = 2$, $\gamma = 0.2$, $a = 0.4$, $b = 0.2$, $\mu = 0.2$, $G_r = 6$, $F = 1$, $P_r = 6.1$, $B_r = 0.3$, $R_d = 1.5$, $x = -2\ to\ 2$, and $y = -2\ to\ 2$].

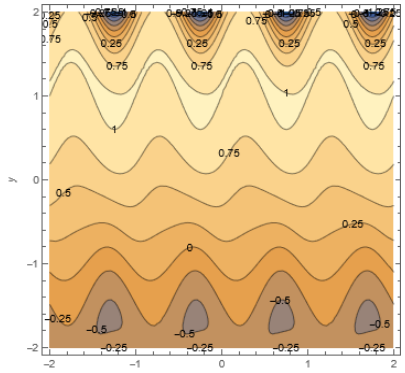

Figure 3.q: Influence of different parameters on stream function [$D_a = 1$, $\phi = \frac{\pi}{6}$, $U = 2$, $\gamma = 0.2$, $a = 0.4$, $b = 0.2$, $\mu = 0.2$, $G_r = 7$, $F = 1$, $P_r = 6.1$, $B_r = 0.3$, $R_d = 1.5$, $x = -2\ to\ 2$, and $y = -2\ to\ 2$].

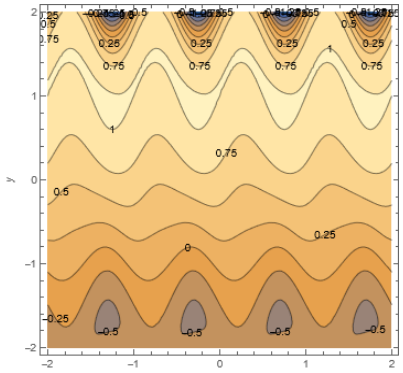

Figure 3.r: Influence of different parameters on stream function [$D_a = 1$, $\phi = \frac{\pi}{6}$, $U = 2$, $\gamma = 0.2$, $a = 0.4$, $b = 0.2$, $\mu = 0.2$, $G_r = 8$, $F = 1$, $P_r = 6.1$, $B_r = 0.3$, $R_d = 1.5$, $x = -2\ to\ 2$, and $y = -2\ to\ 2$].

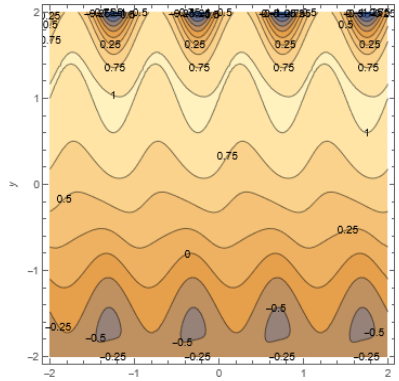

Figure 3.s: Influence of different parameters on stream function [$D_a = 1$, $\phi = \frac{\pi}{6}$, $U = 2$, $\gamma = 0.2$, $a = 0.4$, $b = 0.2$, $\mu = 0.2$, $G_r = 6$, $F = 1$, $P_r = 6.1$, $B_r = 0.3$, $R_d = 1.5$, $x = -2\ to\ 2$, and $y = -2\ to\ 2$].

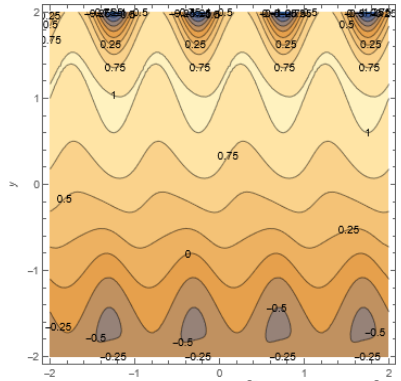

Figure 3.t: Influence of different parameters on stream function [$D_a = 1$, $\phi = \frac{\pi}{6}$, $U = 2$, $\gamma = 0.2$, $a = 0.4$, $b = 0.2$, $\mu = 0.2$, $G_r = 6$, $F = 1$, $P_r = 6.7$, $B_r = 0.3$, $R_d = 1.5$, $x = -2\ to\ 2$, and $y = -2\ to\ 2$].

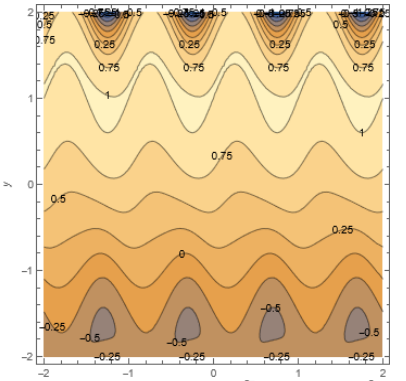

Figure 3.u: Influence of different parameters on stream function [$D_a = 1$, $\phi = \frac{\pi}{6}$, $U = 2$, $\gamma = 0.2$, $a = 0.4$, $b = 0.2$, $\mu = 0.2$, $G_r = 6$, $F = 1$, $P_r = 7$, $B_r = 0.3$, $R_d = 1.5$, $x = -2\ to\ 2$, and $y = -2\ to\ 2$].

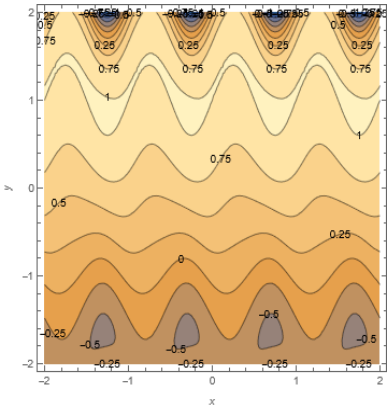

Figure 3.v: Influence of different parameters on stream function [$D_a = 1$, $\phi = \frac{\pi}{6}$, $U = 2$, $\gamma = 0.2$, $a = 0.4$, $b = 0.2$, $\mu = 0.2$, $G_r = 6$, $F = 1$, $P_r = 6.1$, $B_r = 0.3$, $R_d = 1.5$, $x = -2\ to\ 2$, and $y = -2\ to\ 2$].

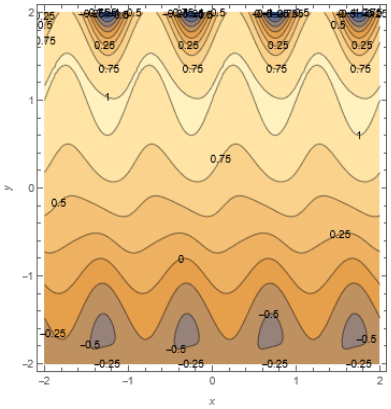

Figure 3.w: Influence of different parameters on stream function [$D_a = 1$, $\phi = \frac{\pi}{6}$, $U = 2$, $\gamma = 0.2$, $a = 0.4$, $b = 0.2$, $\mu = 0.2$, $G_r = 6$, $F = 1$, $P_r = 6.1$, $B_r = 0.3$, $R_d = 2$, $x = -2\ to\ 2$, and $y = -2\ to\ 2$].

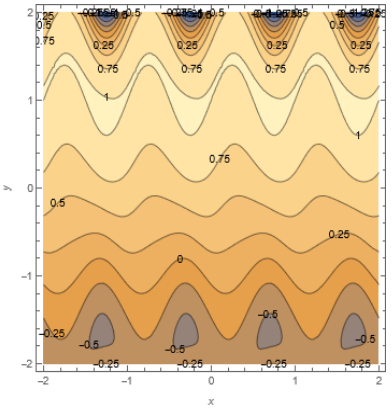

Figure 3.x: Influence of different parameters on stream function [$D_a = 1$, $\phi = \frac{\pi}{6}$, $U = 2$, $\gamma = 0.2$, $a = 0.4$, $b = 0.2$, $\mu = 0.2$, $G_r = 6$, $F = 1$, $P_r = 6.1$, $B_r = 0.3$, $R_d = 2.5$, $x = -2\ to\ 2$, and $y = -2\ to\ 2$].

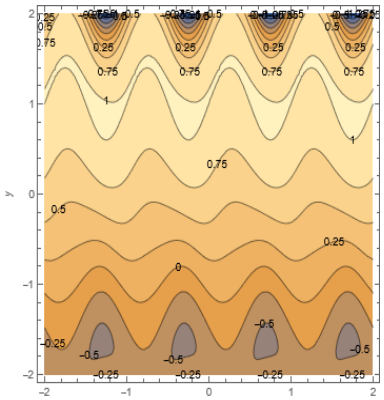

Figure 3.y: Influence of different parameters on stream function [$D_a = 1$, $\phi = \frac{\pi}{6}$, $U = 2$, $\gamma = 0.2$, $a = 0.4$, $b = 0.2$, $\mu = 0.2$, $G_r = 6$, $F = 1$, $P_r = 6.1$, $B_r = 0.3$, $R_d = 1.5$, $x = -2\ to\ 2$, and $y = -2\ to\ 2$].

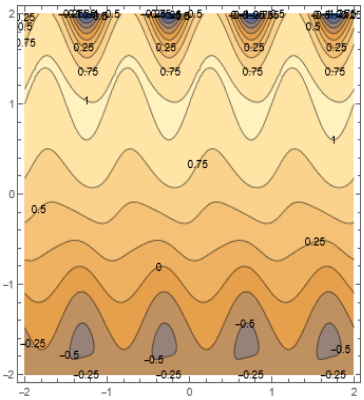

Figure 3.z: Influence of different parameters on stream function [$D_a = 1$, $\phi = \frac{\pi}{6}$, $U = 2$, $\gamma = 0.2$, $a = 0.4$, $b = 0.2$, $\mu = 0.2$, $G_r = 6$, $F = 1$, $P_r = 6.1$, $B_r = 0.5$, $R_d = 1.5$, $x = -2\ to\ 2$, and $y = -2\ to\ 2$].

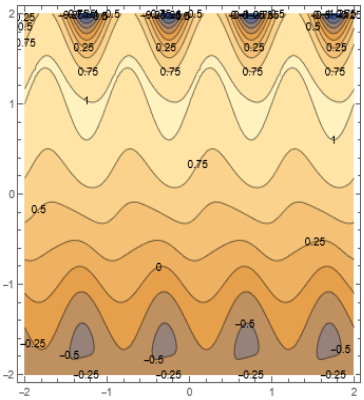

Figure 3.aa: Influence of different parameters on stream function [$D_a = 1$, $\phi = \frac{\pi}{6}$, $U = 2$, $\gamma = 0.2$, $a = 0.4$, $b = 0.2$, $\mu = 0.2$, $G_r = 6$, $F = 1$, $P_r = 6.1$, $B_r = 0.7$, $R_d = 1.5$, $x = -2\ to\ 2$, and $y = -2\ to\ 2$].

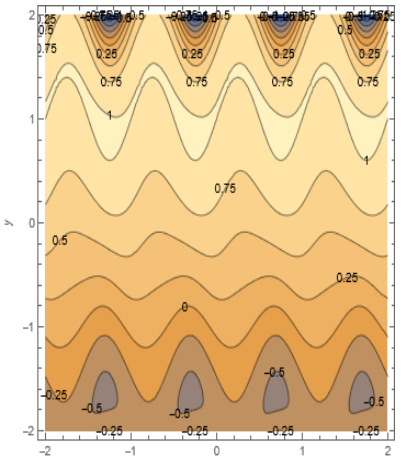

Figure 3.ab: Influence of different parameters on stream function [$D_a = 1$, $\phi = \frac{\pi}{6}$, $U = 2$, $\gamma = 0.2$, $a = 0.4$, $b = 0.2$, $\mu = 0.2$, $G_r = 6$, $F = 1$, $P_r = 6.1$, $B_r = 0.3$, $R_d = 1.5$, $x = -2\ to\ 2$, and $y = -2\ to\ 2$].

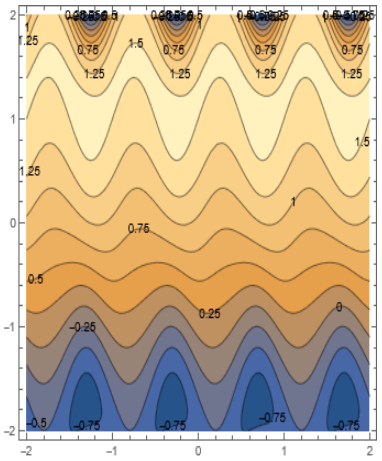

Figure 3.ac: Influence of different parameters on stream function [$D_a = 1$, $\phi = \frac{\pi}{6}$, $U = 2$, $\gamma = 0.2$, $a = 0.4$, $b = 0.2$, $\mu = 0.2$, $G_r = 6$, $F = 1.5$, $P_r = 6.1$, $B_r = 0.3$, $R_d = 1.5$, $x = -2\ to\ 2$, and $y = -2\ to\ 2$].

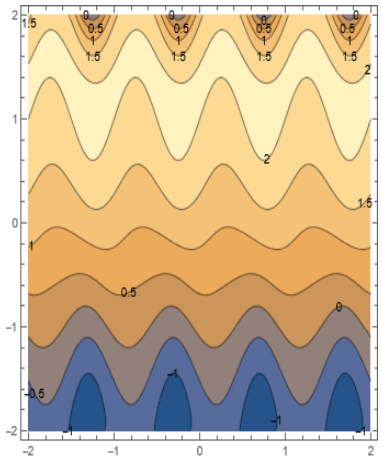

Figure 3.ad: Influence of different parameters on stream function [$D_a = 1$, $\phi = \frac{\pi}{6}$, $U = 2$, $\gamma = 0.2$, $a = 0.4$, $b = 0.2$, $\mu = 0.2$, $G_r = 6$, $F = 2$, $P_r = 6.1$, $B_r = 0.3$, $R_d = 1.5$, $x = -2\ to\ 2$, and $y = -2\ to\ 2$].

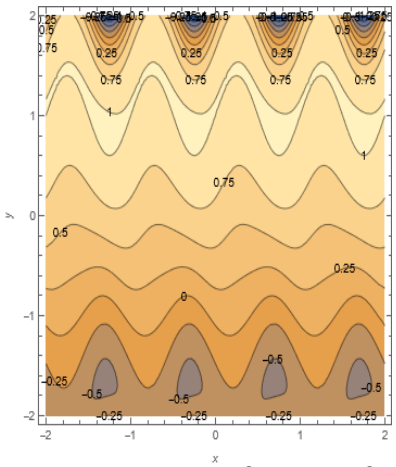

Figure 3.ae: Influence of different parameters on stream function [$D_a = 1$, $\phi = \frac{\pi}{6}$, $U = 2$, $\gamma = 0.2$, $a = 0.4$, $b = 0.2$, $\mu = 0.2$, $G_r = 6$, $F = 1$, $P_r = 6.1$, $B_r = 0.3$, $R_d = 1.5$, $x = -2\ to\ 2$, and $y = -2\ to\ 2$].

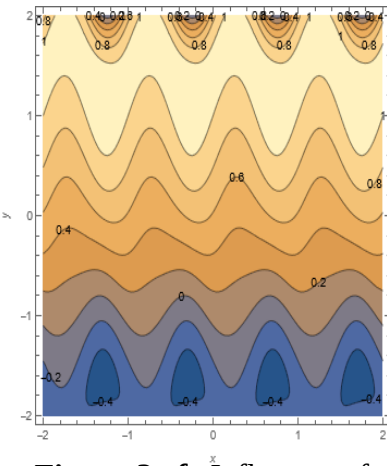

Figure 3.af: Influence of different parameters on stream function [$D_a = 1$, $\phi = \frac{\pi}{6}$, $U = 2$, $\gamma = 0.5$, $a = 0.4$, $b = 0.2$, $\mu = 0.2$, $G_r = 6$, $F = 1$, $P_r = 6.1$, $B_r = 0.3$, $R_d = 1.5$, $x = -2\ to\ 2$, and $y = -2\ to\ 2$].

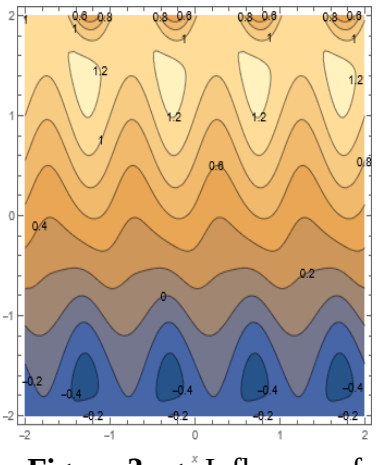

Figure 3.ag: Influence of different parameters on stream function [$D_a = 1$, $\phi = \frac{\pi}{6}$, $U = 2$, $\gamma = 1$, $a = 0.4$, $b = 0.2$, $\mu = 0.2$, $G_r = 6$, $F = 1$, $P_r = 6.1$, $B_r = 0.3$, $R_d = 1.5$, $x = -2\ to\ 2$, and $y = -2\ to\ 2$].

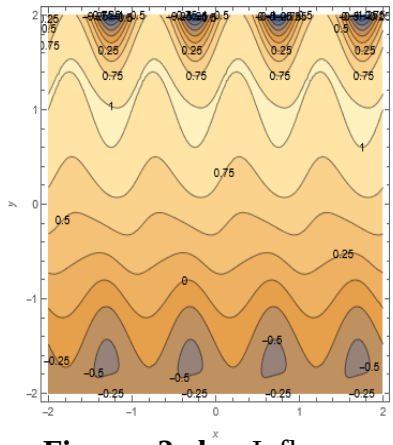

Figure 3.ah: Influence of different parameters on stream function [$D_a = 1$, $\phi = \frac{\pi}{6}$, $U = 2$, $\gamma = 0.2$, $a = 0.4$, $b = 0.2$, $\mu = 0.2$, $G_r = 6$, $F = 1$, $P_r = 6.1$, $B_r = 0.3$, $R_d = 1.5$, $x = -2\ to\ 2$, and $y = -2\ to\ 2$].

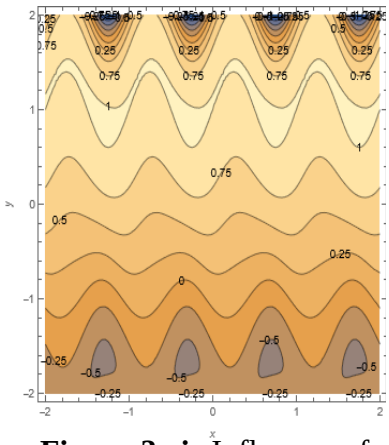

Figure 3.ai: Influence of different parameters on stream function [$D_a = 1$, $\phi = \frac{\pi}{6}$, $U = 2$, $\gamma = 0.2$, $a = 0.4$, $b = 0.2$, $\mu = 0.5$, $G_r = 6$, $F = 1$, $P_r = 6.1$, $B_r = 0.3$, $R_d = 1.5$, $x = -2\ to\ 2$, and $y = -2\ to\ 2$].

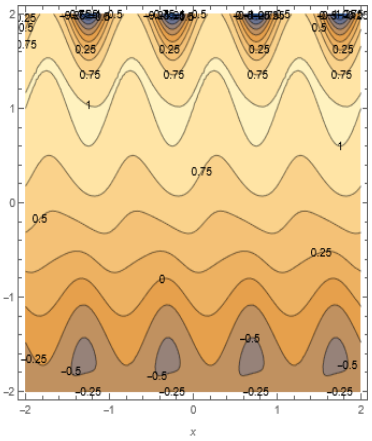

Figure 3.aj: Influence of different parameters on stream function [$D_a = 1$, $\phi = \frac{\pi}{6}$, $U = 2$, $\gamma = 0.2$, $a = 0.4$, $b = 0.2$, $\mu = 1$, $G_r = 6$, $F = 1$, $P_r = 6.1$, $B_r = 0.3$, $R_d = 1.5$, $x = -2\ to\ 2$, and $y = -2\ to\ 2$].

Figure 3: Influence of different parameters on stream function [Φ, D_a, U, γ, a, b, μ, G_r, F, P_r, B_r, R_d, and x=1].

9.3 Behaviour of Pressure Gradient

The difference in the pressure profile and the results that obtained for the effect of some different physical parameters are illustrated in Figures 4.a – 4.l, we can see that the pressure gradient enhanced if the following values of (D_a), (Φ), (a), and (γ) have been increased respectively. But, the pressure gradient decay if (U), (b), (G_r), (F), and (μ) increases, see Figure 4.a, Figure 4.b, Figure 4.d, Figure 4.k, Figure 4.c, Figure 4.e, Figure 4.f, Figure 4.j, and Figure 4.l. While, Figure 4.g, Figure 4.h, and Figure 4.i, show that the pressure gradient (ΔP) goes to increase in the lower wall and it is decay at the upper wall, when (P_r), (R_d), and (B_r) increases. The following figures drawn for explain this behaviour.

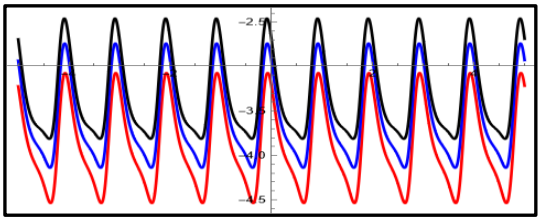

Figure 4.a: Pressure gradient versus axial distance y with different parameters [$D_a = 1, 1.1\ and\ 1.2$, $\phi = \frac{\pi}{6}$, $U = 2$, $\gamma = 0.2$, $a = 0.4$, $b = 0.2$, $\mu = 0.2$, $G_r = 6$, $F = 1$, $P_r = 6.1$, $B_r = 0.3$, $R_d = 1.5$, and $y = 1$].

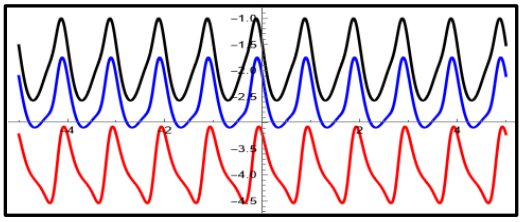

Figure 4.b: Pressure gradient versus axial distance y with different parameters [$D_a = 1$, $\phi = \frac{\pi}{6}, \frac{\pi}{7}\ and\ \frac{\pi}{8}$, $U = 2$, $\gamma = 0.2$, $a = 0.4$, $b = 0.2$, $\mu = 0.2$, $G_r = 6$, $F = 1$, $P_r = 6.1$, $B_r = 0.3$, $R_d = 1.5$, and $y = 1$].

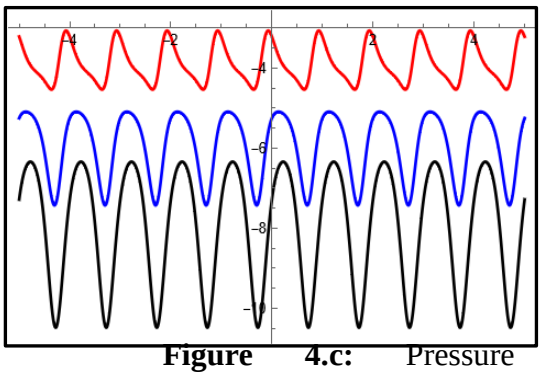

Figure 4.c: Pressure gradient versus axial distance y with different parameters [$D_a = 1$, $\phi = \frac{\pi}{6}$, $U = 2, 1\ and\ 0$, $\gamma = 0.2$, $a = 0.4$, $b = 0.2$, $\mu = 0.2$, $G_r = 6$, $F = 1$, $P_r = 6.1$, $B_r = 0.3$, $R_d = 1.5$, and $y = 1$].

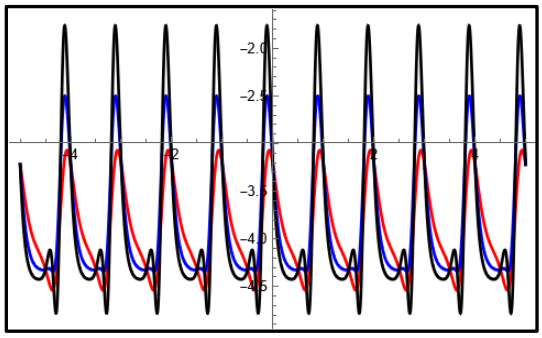

Figure 4.d: Pressure gradient versus axial distance y with different parameters [$D_a = 1$, $\phi = \frac{\pi}{6}$, $U = 2$, $\gamma = 0.2$, $a = 0.4, 0.6\ and\ 0.8$, $b = 0.2$, $\mu = 0.2$, $G_r = 6$, $F = 1$, $P_r = 6.1$, $B_r = 0.3$, $R_d = 1.5$, and $y = 1$].

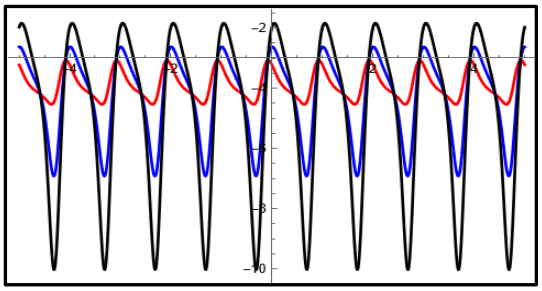

Figure 4.e: Pressure gradient versus axial distance y with different parameters [$D_a = 1$, $\phi = \frac{\pi}{6}$, $U = 2$, $\gamma = 0.2$, $a = 0.4$, $b = 0.2, 0.4\ and\ 0.6$, $\mu = 0.2$, $G_r = 6$, $F = 1$, $P_r = 6.1$, $B_r = 0.3$, $R_d = 1.5$, and $y = 1$].

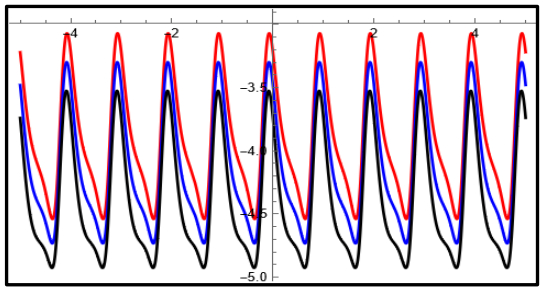

Figure 4.f: Pressure gradient versus axial distance y with different parameters [$D_a = 1$, $\phi = \frac{\pi}{6}$, $U = 2$, $\gamma = 0.2$, $a = 0.4$, $b = 0.2$, $\mu = 0.2$, $G_r = 6, 7\ and\ 8$, $F = 1$, $P_r = 6.1$, $B_r = 0.3$, $R_d = 1.5$, and $y = 1$].

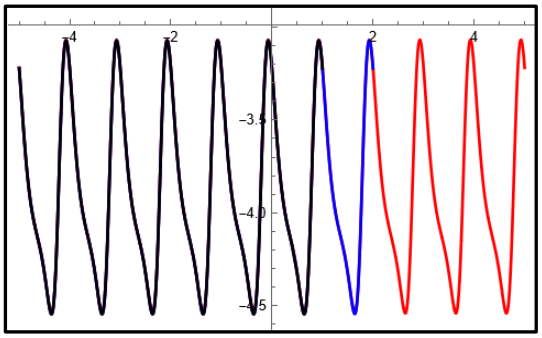

Figure 4.g: Pressure gradient versus axial distance y with different parameters $[D_a = 1,\ \phi = \frac{\pi}{6},\ U = 2,\ \gamma = 0.2,\ a = 0.4,\ b = 0.2,\ \mu = 0.2,\ G_r = 6,\ F = 1,\ P_r = 6.1, 6.7\ and\ 7,\ B_r = 0.3,\ R_d = 1.5,$ and $y = 1]$.

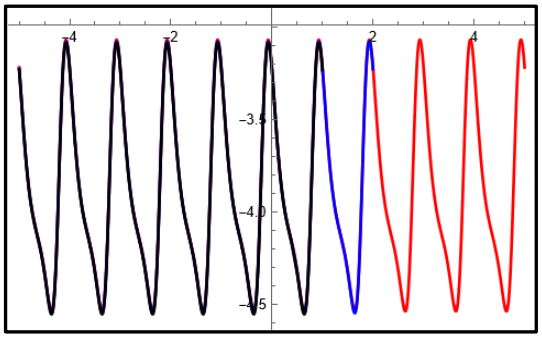

Figure 4.h: Pressure gradient versus axial distance y with different parameters $[D_a = 1,\ \phi = \frac{\pi}{6},\ U = 2,\ \gamma = 0.2,\ a = 0.4, b = 0.2, \mu = 0.2,\ G_r = 6,\ F = 1,\ P_r = 6.1,\ B_r = 0.3,\ R_d = 1.5, 2\ and\ 2.5,$ and $y =$

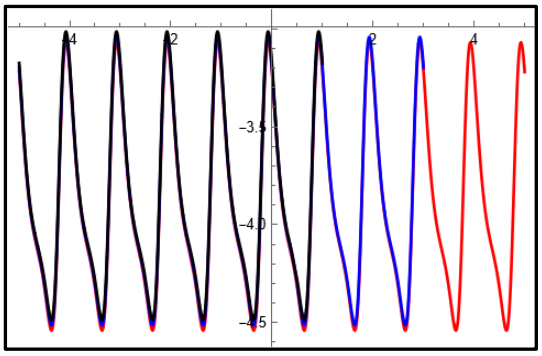

Figure 4.i: Pressure gradient versus axial distance y with different parameters $[D_a = 1,\ \phi = \frac{\pi}{6},\ U = 2,\ \gamma = 0.2,\ a = 0.4,\ b = 0.2,\ \mu = 0.2,\ G_r = 6,\ F = 1,\ P_r = 6.1,\ B_r = 0.3, 0.5\ and\ 0.7,\ R_d = 1.5,$ and $y = 1]$.

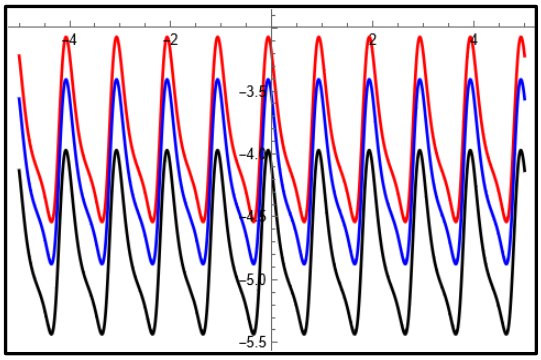

Figure 4.l: Pressure gradient versus axial distance y with different parameters $[D_a = 1,\ \phi = \frac{\pi}{6},\ U = 2,\ \gamma = 0.2,\ a = 0.4,\ b = 0.2,\ \mu = 0.2, 0.5\ and\ 1,\ G_r = 6,\ F = 1,\ P_r = 6.1,\ B_r = 0.3,\ R_d = 1.5,$ and $y = 1]$.

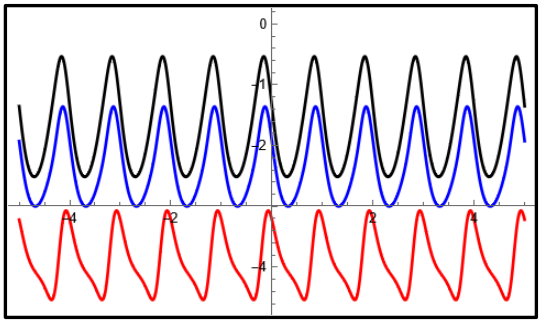

Figure 4.k: Pressure gradient versus axial distance y with different parameters [$D_a = 1$, $\phi = \frac{\pi}{6}$, $U = 2$, $\gamma = 0.2, 0.5\ and\ 1$, $a = 0.4$, $b = 0.2$, $\mu = 0.2$, $G_r = 6$, $F = 1$, $P_r = 6.1$, $B_r = 0.3$, $R_d = 1.5$, and $y = 1$].

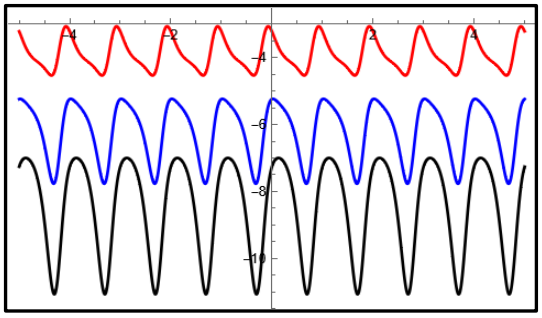

Figure 4.j: Pressure gradient versus axial distance y with different parameters [$D_a = 1$, $\phi = \frac{\pi}{6}$, $U = 2$, $\gamma = 0.2$, $a = 0.4$, $b = 0.2$, $\mu = 0.2$, $G_r = 6$, $F = 1, 1.5\ and\ 2$, $P_r = 6.1$, $B_r = 0.3$, $R_d = 1.5$, and $y = 1$].

Figure 4: Pressure gradient versus axial distance y with different parameters [D_a, Φ, U, γ, a, b, μ, G_r, F, P_r, B_r, R_d, and x=1].

10. Concluding Remarks

In this research, we investigated the electroosmosis augmented MHD peristaltic transport of SWCNTs suspension in porous media as well as effects of non-slip conditions in an asymmetric channel. A long wavelength with low Reynolds number approximations are adopted. A regular perturbation method for small values of Brinkman number is employed to obtain the expression for stream function, temperature and pressure gradient. The effects of Prandtl number (P_r), wave amplitudes (a) and (b), phase difference (Φ), and others are also investigated in details, it found that:

1. The profiles of temperature distribution are parabolic under the impact of all parameters.
2. The temperature coefficient is increased with an increase of (D_a), (U), (a), (b), (μ), (G_r), (F), and (B_r), and decrease with an increase of (Φ), (γ), (P_r), and (R_d).
3. The temperature distribution is rise up at the center region or a "core" of the channel with an increase of (D_a), (U), (b), and (G_r).
4. The effect of (U) is appeared when the parameter (Φ) decreases, in this case, the temperature increases.
5. The size of trapped bolus increase with an increase of (U), (D_a), (a), (b), (G_r), (P_r), (B_r), and (γ) while it is decrease with an increase of (Φ), (R_d), and (μ).
6. The number and size of bolus is rise up with an increase of (F) and (γ). But, the conversely statement is seen with an increase of (Φ), (R_d), and (μ).
7. The pressure gradient increase in magnitude with an increase of (Φ), (D_a), (a), and (γ), and decrease with an increase of (U), (b), (G_r), (F), and (μ). But, the impact of other patient parameters is oscillatory or vacillating.
8. The pressure gradient goes to increase in lower wall while it is decay in upper wall when (P_r), (R_d), and (B_r) increase.

References

[1] S, Noreen; A, Waheed; D, Lu;, "Entropy Analysis in Double-Diffusive Convection in Nanofluids through Electro-Osmotically Induced Peristaltic Microchannel," *Entropy,* vol. 21, p. 986, 2019.

[2] S, Noreen; A, Riaz; D, Lu;, "Soret-Dufour Effects in Electroosmotic Biorheological Flow of Jeffrey Fluid," *Heat Transfer, Wiley Periodicals, Inc.,* vol. 1, pp. 7540-7585, 2020.

[3] M. A. Murad and A. M. Abdulhadi, "Influence of Heat and Mass Transfer on Peristaltic Transport of Viscoplastic Fluid in Presence of Magnetic Field through Symmetric Channel with Porous Medium," in *J. Phys.: Conf. Ser. 1804012060,* 2021.

[4] F. A. Adnan and A. M. Abdulhadi, "Effect of a Magnetic Field on Peristaltic Transport of Bingham Plastic Fluid in a Symmetric Channel," *Sci. Int. Lahore,* vol. 311, pp. 29-40, 2019.

[5] T. Hayat, R. Ellahi and F. M. Mahomed, "The Analytical Solutions for Magnetohydrodynamic Flow of a Third Order Fluid in a Porous Medium," *Zeitschrift für Naturforschung A,* vol. 64, no. 9-10, pp. 531-539, 2009.

[6] S. S. Hasn and A. M. Abdualhadi, "MHD Effect on Peristaltic Transport for Rabinowitsch Fluid Through A Porous Medium in Cilia Channel," *Iraqi Journal of Sciences,* vol. 616, pp. 1461-1472, 2020.

[7] J. C. Misra, B. Mallick and A. Sinha, "Heat and Mass Transfer in Asymmetric Channels During Peristaltic Transport of an MHD Fluid Having Temperature-Dependent Properties," *Alexandria Engineering Journal,* vol. 57, no. 1, pp. 391-406, 2018.

[8] M. Kothandapani, J. Prakash and V. Pushparaj, "Analysis of Heat and Mass Transport of MHD Peristaltic Flow Through a Tapered Asymmetric Channel," *Journal of fluid,* vol. 2015, p. 9, 2015.

[9] Z. Asghar and N. Ali, "Mixed Convective Heat Transfer Analysis for the Peristaltic Transport of Viscoplastic Fluid: Perturbation and Numerical Study," *AIP Advances ,* vol. 9, p. 095001, 2019.

[10] A. M. Abdualhadi and A. H. Al-Hadad, "Effects of Rotation and MHD on the Nonlinear Peristaltic Flow of A Jeffery Fluid in An Asymmetric Channel Through A Porous Medium," *Iraqi Journal of Sciences,* vol. 57, no. 1 A, pp. 223-240, 2016.

[11] S. Hussain and N. Ali, "Electro-Kinetically Modulated Peristaltic Transport of Multilayered Power Law Fluid in an Axisymmetric Tube," *Eur. Phys. J. Plus,* vol. 135, p. 348, 2020.

[12] S. Sreenadh, P. Lakshminrayana, M. A. Kumar and G. Sucharitha, "Effect of MHD on Peristaltic Transport of a Pseudoplastic Fluid in an Asymmetric Channel with Porous Medium," *IJMSEA,* vol. 8, no. V, pp. 27-40, 2014.

[13] C. Zaho and C. Yang, "Electrokinetics of Non-Newtonian Fluids: A Review," *Adv. Colloid. Interface Sci.,* vol. 201, pp. 94-108, 2013.

[14] A. S. a. e. al., "Mathematical Computations for Peristaltic Flow of Heated Non-Newtonian Fluid Inside a Sinusoidal Elliptic Duct," *Phys. Scr.,* vol. 95, no. 105009, 2020.

[15] M. M. Bahatti, S. Z. Alamri, R. Ellahi and S. I. Abdelsalam, "Intra-Uterine Particle-Fluid Motion Through a Compliant Asymmetric Tapered Channel with Heat Transfer," *Journal of Thermal Analysis and Calorimetry,* vol. 144, no. 6, 2020.

[16] M. R. Salman and A. M. Abdualhadi, "Effects of MHD on Peristalsis Transport and Heat Transfer with Variables Viscosity in Porous Medium," *International Journal of Science*

and Research (IJSR), vol. 7, no. 2, pp. 612-623, 2018.

[17] S. Akram, S. Nadeem and A. Hussain, "Effects of Heat and Mass Transfer on Peristaltic Flow of a Bingham Fluid in the Presence of Inclined Magnetic Field and Channel with Different Wave Forms," *Journal of Magnetism and Magnetic Material*, vol. 362, no. 8, pp. 184-192, 2014.